Ca2+ Extrusion via Na+–Ca2+ Exchangers in Rat Odontoblasts

ARTICLE *in* JOURNAL OF ENDODONTICS · APRIL 2010

Impact Factor: 3.38 · DOI: 10.1016/j.joen.2010.01.006 · Source: PubMed

Ca^{2+} Extrusion via Na^+-Ca^{2+} Exchangers in Rat Odontoblasts

Maki Tsumura, MSc,[,†,‡] Reijiro Okumura, DDS, PhD,[†,§,‖] Shoko Tatsuyama, DDS, PhD,[¶] Hideki Ichikawa, DDS,[*,†] Takashi Muramatsu, DDS, PhD,[*,‖] Toshio Matsuda, PhD,[#] Akemichi Baba, PhD,[**] Keiko Suzuki, DVM,[††] Hiroshi Kajiya, PhD,[‡‡] Yoshinori Sahara, DDS, PhD,[§§,‖‖] Masayuki Tokuda, DDS, PhD,[¶] Yasunori Momose, PhD,[‡] Masakazu Tazaki, DDS, PhD,[*,†] Masaki Shimono, DDS, PhD,[‖] and Yoshiyuki Shibukawa, DDS, PhD[*,†]*

Abstract

Introduction: Intracellular Ca^{2+} is essential to many signal transduction pathways, and its level is tightly regulated by the Ca^{2+} extrusion system in the plasma membrane, which includes the Na^+-Ca^{2+} exchanger (NCX). Although expression of NCX1 isoforms has been demonstrated in odontoblasts, the detailed properties of NCX remain to be clarified. In this study, we investigated localization and ion-transporting/pharmacologic properties of NCX isoforms in rat odontoblasts. **Methods:** We characterized both the reverse and forward modes of NCX activity in odontoblasts in a dental pulp slice preparation. Ca^{2+} influx by reverse NCX activity was measured by fura-2 fluorescence. Ca^{2+} efflux by forward NCX activity elicited inward Na^+ current as measured by perforated-patch clamp recording. For immunohistochemical analysis, cryostat sections of incisors were incubated with antibodies against NCX. **Results:** Immunohistochemical observation revealed localization of NCX1 and NCX3 in the distal membrane of odontoblasts. Inward currents by forward NCX activity showed dependence on external Na^+. Fura-2 fluorescence measurement revealed that Ca^{2+} influx by reverse NCX activity depended on extracellular Ca^{2+} concentration, and that this influx was blocked by NCX inhibitor KB-R7943 in a concentration-dependent manner. However, Ca^{2+} influx by NCX showed a slight sensitivity to SEA0400 (a potent NCX1 inhibitor), indicating that expression potencies in odontoblasts were NCX3 > NCX1. **Conclusions:** These results suggest that odontoblasts express NCX1 and NCX3 at the distal membrane, and that these isoforms play an important role in the Ca^{2+} extrusion system as well as in the directional Ca^{2+} transport pathway from the circulation to the dentin-mineralizing front. *(J Endod 2010;36:668–674)*

Key Words

Ca^{2+} signaling, channel, intracellular Ca^{2+} concentration, Na^+-Ca^{2+} exchanger, odontoblast, patch-clamp

The plasma membrane Na^+-Ca^{2+} exchanger (NCX) is a bidirectional transporter that catalyzes the electrogenic exchange of 3 or 4 Na^+ for 1 Ca^{2+}, depending on the electrical and chemical gradients of the substrate ions (1–4). The NCX plays a critical role in the regulation of intracellular Ca^{2+} concentrations ($[Ca^{2+}]_i$) in both excitable and nonexcitable cells and is mainly thought to pump Ca^{2+} to the outside of the cell by using the Na^+ concentration gradient across the cell membrane (1, 2). Mammalian NCX belongs to the multigene family SLC8A, which comprises NCX1, NCX2, and NCX3 (5). Whereas the various isoforms of NCX1 are almost ubiquitously expressed (in organs such as the heart, brain, and kidney and at lower levels in other tissues as well), expression of NCX2 and NCX3 is limited mainly to the brain and skeletal muscle (5).

Dentin formation and mineralization are achieved by transcellular transport of Ca^{2+} by odontoblasts, and the Ca^{2+} transporting mechanisms are mediated by Ca^{2+} influx, mobilization, and extrusion mechanisms (6–10). Odontoblasts have been reported to express various Ca^{2+} mobilization/signaling pathways, including Ca^{2+} release from intracellular Ca^{2+} stores and Ca^{2+} influx from the extracellular medium via plasma membrane Ca^{2+} channels (10–14). At the same time, intracellular Ca^{2+} levels are tightly regulated by continuous removal of excess internal Ca^{2+} via Ca^{2+}–adenosine triphosphatase (PMCA) and/or NCX in the plasma membrane. Expression of both PMCA and NCX1 isoforms has been demonstrated in dentinogenetically active odontoblasts and is considered to be involved in dentin mineralization by exclusion of Ca^{2+} to the mineralizing front (6, 7, 9, 15). It has been reported that NCX has a 10-fold lower affinity for Ca^{2+} but a 10-fold to 50-fold higher turnover rate than

From the *Oral Health Science Center, Tokyo Dental College, Chiba, Japan; †Department of Physiology, Tokyo Dental College, Chiba, Japan; ‡Department of Clinical Pharmacy, Faculty of Pharmaceutical Sciences, Toho University, Funabashi, Japan; §Department of Endodontics, Pulp and Periapical Biology, Tokyo Dental College, Chiba, Japan; ‖Department of Pathology, Tokyo Dental College, Chiba, Japan; ¶Department of Restorative Dentistry and Endodontology, Kagoshima University Graduate School of Medical and Dental Sciences, Kagoshima, Japan; #Laboratory of Medicinal Pharmacology, Graduate School of Pharmaceutical Sciences, Osaka University, Osaka, Japan; **Laboratory of Molecular Neuropharmacology, Graduate School of Pharmaceutical Sciences, Osaka University, Osaka, Japan; ††Southern Alberta Cancer Research Institute, Department of Biochemistry and Molecular Biology, Faculty of Medicine, University of Calgary, Calgary, AB, Canada; ‡‡Department of Physiological Science and Molecular Biology, Fukuoka Dental College, Fukuoka, Japan; §§Department of Physiology, Tsurumi University School of Dental Medicine, Yokohama, Japan; and ‖‖Department of Oral Physiology, School of Dentistry, Iwate Medical University, Morioka, Japan.

Drs Tsumura, Shibukawa, and Okumura contributed equally to this work.

Address requests for reprints to Dr Yoshiyuki Shibukawa, Department of Physiology, Tokyo Dental College, 1-2-2, Masago, Mihama-ku, Chiba-city, Chiba 261-8502, Japan. E-mail address: yshibuka@tdc.ac.jp.

0099-2399/$0 - see front matter

doi:10.1016/j.joen.2010.01.006

PMCA. The high turnover rate of the NCX is important in cells that need to extrude large amounts of Ca^{2+} (2).

To clarify the dynamic features of Ca^{2+} extrusion underlying regulation of intracellular Ca^{2+} levels and the mechanism of dentin formation in odontoblasts, we directly measured Na^+-Ca^{2+} exchange activity and determined the biophysical and pharmacologic profile of NCX in odontoblasts. Members of the NCX family, as bidirectional transporters, carry out either Ca^{2+} efflux or influx (Ca^{2+} efflux by forward exchange or Ca^{2+} influx by reverse exchange), depending on the direction of the transmembrane Na^+ gradient. Therefore, we performed patch-clamp recording to measure Ca^{2+} efflux by forward NCX activity and fura-2 fluorescence imaging to measure Ca^{2+} influx by reverse NCX activity. In addition, we investigated localization of NCX in odontoblasts.

Materials and Methods

Dental Pulp Slice Preparations

All animals were treated in accordance with the Guiding Principles for the Care and Use of Animals in the Field of Physiological Sciences approved by the Council of the Physiological Society of Japan and the American Physiological Society and with the guidelines established by the National Institutes of Health in the USA regarding the care and use of animals for experimental procedures. The study was approved by the Ethics Committee of Tokyo Dental College.

Dental pulp slice preparations were obtained from a total of 28 newborn Wistar rats by using a previously described method (10, 12–14, 16). Briefly, decapitation was performed under pentobarbital sodium anesthesia, and the mandible was dissected. Hemimandibles embedded in alginate impression material were sectioned transversely through the incisor at 500 μm in thickness by using a standard vibrating tissue slicer (DTK-100; Dosaka EM, Kyoto, Japan). Sections of mandible were sliced down to the required level at which the dentin and enamel were directly visible between the bone tissue and dental pulp. Then the surrounding impression material, bone tissue, enamel, and dentin were removed carefully, and the remaining dental pulp slice was obtained. Pulp slices were treated with a standard solution containing collagenase and trypsin at 37°C for 30 minutes to obtain acutely isolated odontoblasts. For $[Ca^{2+}]_i$ measurement and patch-clamp recordings, isolated odontoblasts were plated onto a culture dish and bathed in minimum essential medium (Invitrogen, Grand Island, NY) containing 10% fetal bovine serum and 5% horse serum and maintained at 37°C in a 5% CO_2 incubator. Recording solutions and drugs were applied by superfusion over the dental pulp slice by using a rapid gravity-fed perfusion system (VC-6 or 8; Warner Instruments, Hamden, CT). Solution changes were completed within ~20 milliseconds. These primary cultured cells were used within 24 hours. Cells localized on the rim of the primary cultured dental pulp slice were chosen for $[Ca^{2+}]_i$ measurement and patch-clamp recordings.

Whole-Cell Recording Techniques

Whole-cell recordings were carried out by using a nystatin perforated-patch recording configuration under voltage-clamp conditions (17). Patch pipettes with a resistance of 2–5 MΩ were pulled from capillary tubes by using a Flaming/Brown micropipette puller (Model P80/PC; Sutter Instrument, Novato, CA) and filled with a pipette solution containing nystatin. Whole-cell currents were measured by using a patch-clamp amplifier (L/M-EPC-7+; Heka Elektronik, Lambrecht, Germany). Current traces were displayed and stored in a computer by using pCLAMP (Axon Instruments, Foster City, CA) after digitizing the analogue signals at 0.5 kHz (DigiData 1440A; Axon Instruments). Current records were filtered at 10 Hz. Data were analyzed offline by using pCLAMP and a technical graphics/analysis program (ORIGIN; MicroCal Software, Northampton, MA). The Ca^{2+} efflux by forward Na^+-Ca^{2+} exchange currents was recorded with a holding potential of 0 mV.

Measurement of Ca^{2+}-Sensitive Dye Fluorescence

The dental pulp slices were incubated for 30 minutes at 37°C in the standard solution containing 10 μmol/L fura-2 acetoxymethyl ester (Dojindo Laboratories, Kumamoto, Japan) and 0.1% (w/v) pluronic acid F-127 (Molecular Probes, Eugene, OR), followed by rinsing with fresh standard solution. A dish with fura-2–loaded odontoblasts was mounted on the stage of a microscope (Olympus, Tokyo, Japan) incorporated into the Aquacosmos system and software (Hamamatsu Photonic, Shizuoka, Japan) equipped with an excitation wavelength selector and an intensified charge-coupled device camera. $[Ca^{2+}]_i$ was expressed as the fluorescence ratio ($R_{F340/F380}$) at 2 excitation wavelengths of 380 nm and 340 nm.

Immunofluorescence Analysis

Mandibles were dissected from 7-day-old Wistar rats anesthetized with pentobarbital sodium. Mandibles were embedded in OCT compound (TissueTek, Elkhart, IL), rapidly frozen in isopentane (–80°C), and sagittally sectioned (together with mandibular incisors) to 6 μm in thickness without decalcification. These cryosections were mounted on glass slides at –20°C (Matsunami, Osaka, Japan). To identify NCX isoform localization, after blocking in 10% goat or rabbit serum, cryosections were incubated with rabbit anti-NCX1 or goat anti-NCX2 or anti-NCX3 polyclonal antibodies (Santa Cruz Biotechnology, Santa Cruz, CA; dilution 1:100) at 4°C overnight. Primary cultured cells in the dental pulp slice were also incubated with rabbit anti–dentin matrix protein-1 polyclonal antibodies (DMP-1; TaKaRa-Bio, Shiga, Japan) at 4°C overnight. Sections were incubated with a secondary antibody (Alexa Fluor 488 goat anti-rabbit or rabbit anti-goat IgG for NCXs or Alexa Fluor 546 goat anti-rabbit IgG; Molecular Probes; dilution 1:100) for fluorescence staining and with 4′,6-diamino-2-phenylindole (Molecular Probes) for nuclear staining at room temperature for 5 minutes. Negative controls were prepared by using nonimmune IgGs diluted at equivalent concentrations to primary antibodies (data not shown). Sections were examined under a conventional fluorescence microscope (Zeiss, Jena, Germany).

Solutions and Reagents

The standard solution consisted of the following (in mmol/L): 136 NaCl, 5 KCl, 2.5 $CaCl_2$, 0.5 $MgCl_2$, 10 HEPES, and 10 glucose (pH 7.4). For the nystatin-perforated patch recording, extracellular solution contained (in mmol/L) 150 LiCl, 1 ethylenediaminetetraacetic acid (EDTA), 10 sucrose, and 20 HEPES (pH 7.4). To activate the Ca^{2+} efflux by forward NCX activity, extracellular Li^+ concentration ($[Li^+]_o$) with 1 mmol/L EDTA was substituted with equimolar extracellular Na^+ ($[Na^+]_o$) with 0.05 mmol/L EDTA. The intracellular solution contained (in mmol/L) 110 K-glutamate, 20 KCl, 2 Mg-ATP, 20 TEA-Cl, 10 $CaCl_2$, 10 EGTA, and 20 HEPES (pH 7.2). For $[Ca^{2+}]_i$ measurement, the extracellular solution consisted of (in mmol/L) 150 NaCl, 0.02–0.2 $CaCl_2$, 10 sucrose, and 20 HEPES (pH 7.4). To activate Ca^{2+} influx by NCX activity, $[Na^+]_o$ was substituted with equimolar $[Li^+]_o$. Except for those noted above, all reagents were obtained from Sigma Chemical Co (St Louis, MO). SEA0400 (2-[4-[(2,5-difluorophenyl)methoxy]phenoxy]-5-ethoxyaniline) was synthesized by Taisho Pharmaceutical Co Ltd (Saitama, Japan) (18).

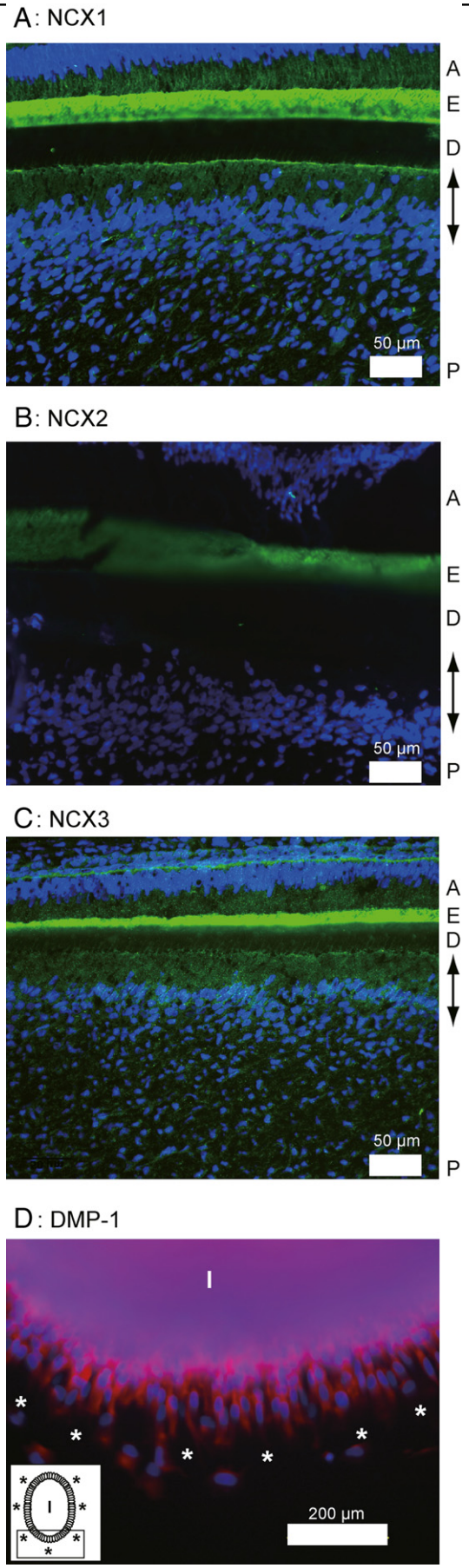

Statistics and Offline Analysis

The Ca^{2+}- and Na^+-dependence of Na^+-Ca^{2+} exchange was obtained by fitting the data with the function:

$$A = A_{max} / \left[1 + \left(K/[x]_o\right)^h\right] + A_{min} \qquad \text{(equation 1)}$$

where K is the equilibrium binding constant for applied $[Ca^{2+}]_o$ with a Hill coefficient (h) equal to 1 or the apparent dissociation constant for applied $[Na^+]_o$. The dose-response relationship for inhibitory effects of NCX inhibitors was obtained by fitting the data with the function:

$$A = A_{max} / \left[1 + 10^{\left([x]_o - \log[IC50]\right)}\right] + A_{min} \qquad \text{(equation 2)}$$

where IC_{50} is 50% inhibitory concentration for applied NCX inhibitors. A_{max} is maximal, and A_{min} is minimal response. The $[x]_o$ indicates applied concentration of extracellular Ca^{2+}, Na^+, or inhibitors.

Data were expressed as the mean ± standard error (SE) of the mean of the values for tested cells (n). Paired *t* tests (two-sided) were used to determine statistical significance. *P* values of less than .05 were considered significant.

Results

Localization of NCX in Odontoblasts

Immunohistochemical observation revealed NCX-positive (green), tall, columnar odontoblasts (Fig. 1) during dentin formation. Immunoreactivity for NCX1 (Fig. 1*A*) and NCX3 (Fig. 1*C*), but not NCX2 (Fig. 1*B*), was observed. Strong immunoreaction was found on the distal plasma membrane of odontoblasts adjacent to the internal dentin surface.

Ca^{2+}- and Na^+-Dependence of Na^+-Ca^{2+} Exchange in Odontoblasts

Odontoblasts located at the rim of the dental pulp slices were loaded with fura-2, and $[Ca^{2+}]_i$ was measured. The cells were identified as odontoblasts on the basis of their distinct immunoreactivity. The cells also exhibited dentin matrix protein (DMP)-1–positive staining (asterisks in Fig. 1*D*), indicating that they were odontoblasts (19, 20). The $[Ca^{2+}]_i$ response in odontoblasts was expressed as F/F_0 units, and the $R_{F340/F380}$ value (*F*) was normalized to the resting value (F_0). Members of the NCX gene family have been shown to perform either Ca^{2+} efflux or Ca^{2+} influx, depending on the direction of the transmembrane Na^+ gradient (2, 21). Ca^{2+} influx in exchange for intracellular Na^+ is readily observed on removal of extracellular Na^+ and is referred to as the Ca^{2+} influx by reverse NCX activity. In the present study, the cells

Figure 1. Immunohistochemical localization of NCXs and DMP-1. (*A–C*) NCX immunoreaction (green) and nuclei (blue). Odontoblasts are tall and columnar. Intense immunoreactivity is observed for NCX1 (*A*) and NCX3 (*C*) at distal ends of odontoblast membrane, whereas no immunoreaction is observed for NCX2 (*B*). Arrows indicate odontoblast layer. A, ameloblast layer; E, enamel; D, dentin; P, dental pulp. Scale bars: 50 μm. (*D*) DMP-1 immunoreaction (red) and nuclei (blue). Inset at bottom left shows schematic of dental pulp slice. Box in inset represents observation area for (*D*). DMP-1–positive odontoblasts (asterisks in (*D*) and inset) at rim of dental pulp slice are observed emerging from inner area of dental pulp (I). Scale bar: 200 μm. No fluorescence is detected in negative control (not shown). NCX and DMP-1 immunoreaction patterns were consistently observed in 3 mandibles and 4 primary cultured dental pulp slices, respectively.

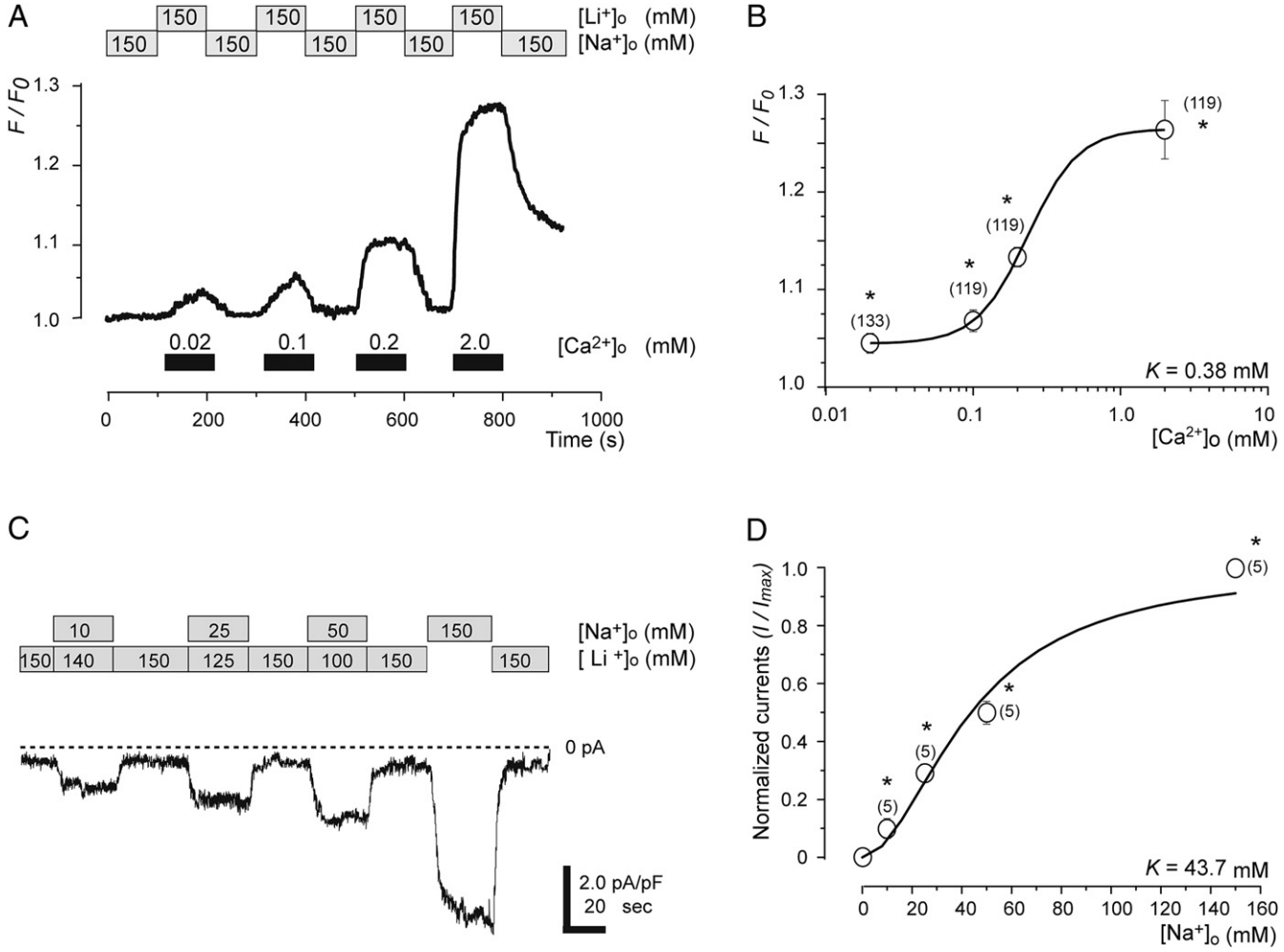

Figure 2. Ca^{2+} (*A, B*) and Na^+ (*C, D*) dependence of NCX expressed in odontoblasts. (*A*) Ca^{2+} influx by NCX in odontoblasts activated by substituting Na^+-containing external solution with Li^+-containing solution while maintaining osmotic strength by replacing NaCl with LiCl. Applied solution-changing protocol for $[Na^+]_o$ and $[Li^+]_o$ is shown in upper panel; protocol for $[Ca^{2+}]_o$ is shown in lower panel. (*B*) Concentration-response relationship for $[Ca^{2+}]_o$. Data points illustrate F/F_0 values as a function of applied concentrations of extracellular Ca^{2+}. Data points represent mean ± SE of a number of tested cells (numbers in parentheses). Curve (solid line) on semilogarithmic scale was fitted to Equation 1 described in text. A_{max} is maximal F/F_0 (1.26); A_{min} is minimal F/F_0 (1.05); h is 1.0. $^*P < .05$; significant differences in F/F_0 values recorded between each combination of 0.02–2.0 mmol/L and 0 mmol/L $[Ca^{2+}]_o$. (*C*) Typical inward Na^+ current via Ca^{2+} efflux by NCX in odontoblasts. These cells were voltage-clamped at a holding potential of 0 mV. Boxes in upper panel indicate protocol of solution changes applied. Forward exchange was activated by substituting Li^+-containing external solution with Na^+-containing solution while maintaining osmotic strength by replacing LiCl with NaCl. (*D*) Concentration-response relationship for $[Na^+]_o$. Data points illustrate current amplitude as function of applied concentrations of extracellular Na^+. Data points represent mean ± SE of a number of tested cells (numbers in parentheses). Curve (solid line) was fitted to Equation 1 described in text. A_{max} is maximal I/I_{max} (1.0); A_{min} is minimal I/I_{max} (0). $^*P < .05$; significant differences in current amplitude recorded between each combination of 10–150 mmol/L and 0 mmol/L $[Na^+]_o$.

were first perfused with medium containing 150 mmol/L Na^+, which was then equimolar-replaced with Li^+ (ie, removal of Na^+) to reverse the Na^+ gradient across the plasma membrane in the presence of extracellular Ca^{2+}. In the odontoblasts, significant increases in $[Ca^{2+}]_i$ caused by Ca^{2+} influx by reverse NCX activity were clearly dependent on extracellular Ca^{2+} concentration ($[Ca^{2+}]_o$) (Fig. 2*A*). Increases in $[Ca^{2+}]_i$ via reverse Na^+-Ca^{2+} exchange were induced by addition of 4 different concentrations of $[Ca^{2+}]_o$ (0.02–2.0 mmol/L). The semilogarithmic plot (Fig. 2*B*) illustrates F/F_0 values as a function of applied $[Ca^{2+}]_o$, with an equilibrium binding constant of 0.38 mmol/L (Fig. 2*B*, solid line).

Further studies were carried out to measure NCX activity directly in DMP-1–positive odontoblasts by using a nystatin perforated-patch recording configuration. An inward current via forward NCX activity was induced by substituting external solution containing 150 mmol/L Li^+ and 1 mmol/L EDTA with external solution containing 10–150 mmol/L Na^+ and 50 μmol/L EDTA. The holding potential was 0 mV. When Li^+ was replaced by Na^+, inward Na^+ currents were observed. The current trace in Fig. 2*C* shows a typical example of the change in inward current that was observed with this series of solution changes at various concentrations (10–150 mmol/L) of external Na^+. Amplitudes of inward current showed an increase, with increasing concentrations of $[Na^+]_o$ ranging from 0–150 mmol/L. The plot in Fig. 2*D* illustrates the inward Na^+ current amplitudes as a function of applied $[Na^+]_o$. Current amplitudes (I/I_{max}) are shown normalized to the current amplitude observed with 150 mmol/L Na^+ medium applied. Inward Na^+ current via forward Na^+-Ca^{2+} exchange depended on external Na^+ concentration, with an apparent dissociation constant of 43.7 mmol/L and a Hill coefficient of 2.0 (Fig. 2*D*; n = 5).

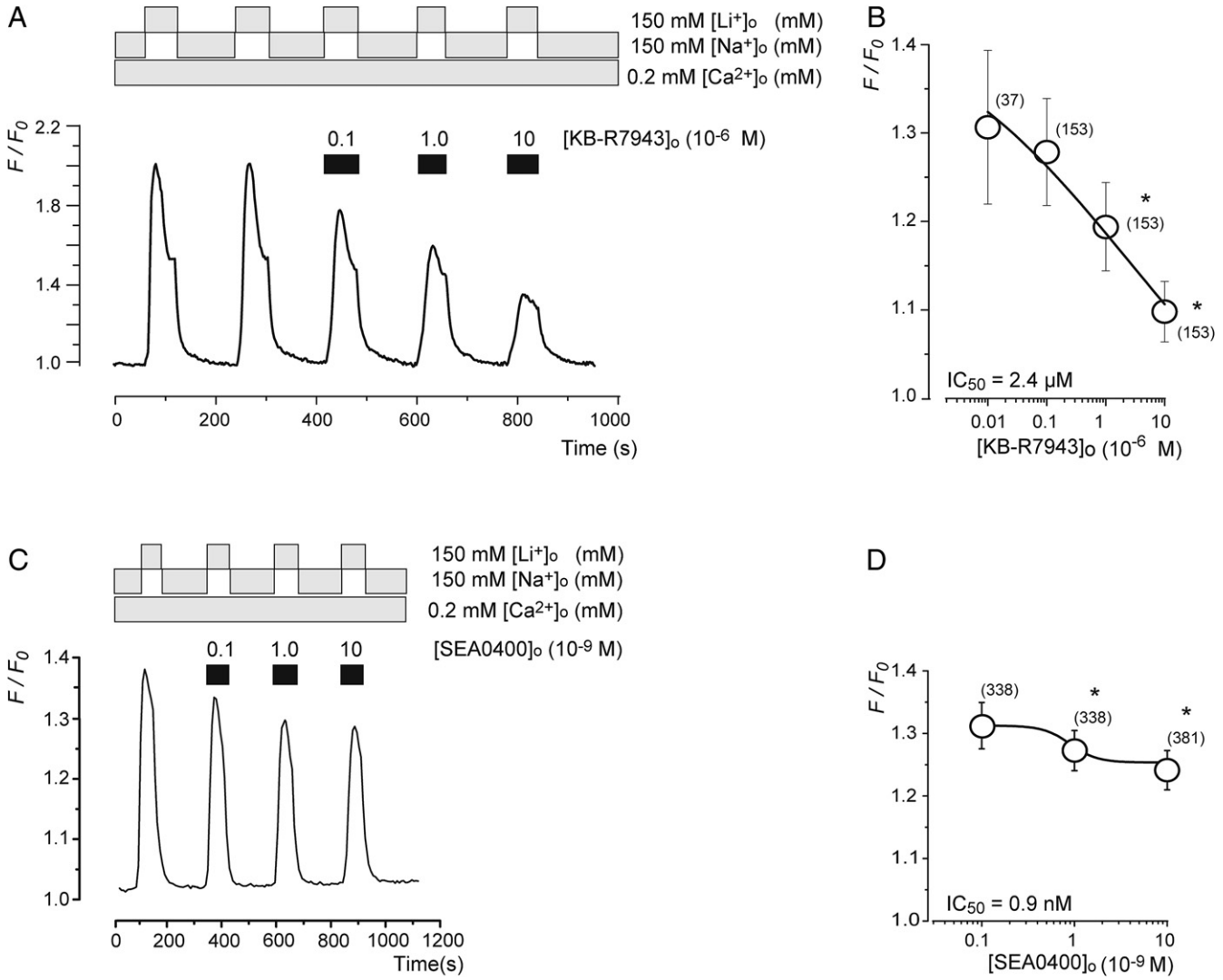

Figure 3. Pharmacologic characteristics of NCX expressed in odontoblasts. Dose-dependent inhibition of NCX by KB-R7943 (*A, B*) and SEA0400 (*C, D*). (*A, C*) Increases in $[Ca^{2+}]_i$ evoked by Ca influx by NCX were reversibly (not shown) inhibited by KB-R7943 (*A*) and SEA0400 (*C*) in a concentration-dependent manner. External solution-changing protocol for $[Na^+]_o$ alone and for $[Li^+]_o$ with 0.2 mmol/L $[Ca^{2+}]_o$ is shown in upper panels of each figure. Black bars in each figure indicate times of addition of these inhibitors to external solution. (*B, D*) Dose-response relationship for inhibitory effects of KB-R7943 (*B*) and SEA0400 (*D*) on Ca^{2+} influx by NCX. Data points in each figure illustrate F/F_0 values as a function of applied concentrations of inhibitors and represent mean ± SE of a number of tested cells (numbers in parentheses). Curves (solid lines) were fitted according to Equation 2 described in text. A_{max} is maximal F/F_0; A_{min} is minimal F/F_0. *$P <$ .05; significant differences in F/F_0 values between values recorded before and after application of each concentration of inhibitors.

Pharmacologic Identification of NCX Isoforms in Odontoblasts

To determine the pharmacologic profile of the expressed NCX, the effects of KB-R7943 and SEA0400 on Ca^{2+} influx by NCX were investigated. In the presence of 0.2 mmol/L $[Ca^{2+}]_o$, application of KB-R7943 significantly blocked Ca^{2+} influx by reverse NCX activity (Fig. 3*A*), whereas application of SEA0400 showed only a small but significant inhibition of Ca^{2+} influx (Fig. 3*C*). A 50% blockage of inhibitory concentration (IC_{50}) was obtained at a KB-R7943 concentration of 2.4 μmol/L (Fig. 3*B*) and an SEA0400 concentration of 0.9 nmol/L (Fig. 3*D*).

Discussion

Our biophysical/pharmacologic and immunohistochemical analyses in rat odontoblasts clarified functional NCX1 and NCX3 expression in the distal membrane adjacent to the internal dentin surface. Earlier studies found that benzyloxyphenyl derivatives KB-R7943 and SEA0400 specifically inhibited NCX, and that they particularly inhibited Ca^{2+} influx by reverse NCX activity (4, 22). The values of IC_{50} for KB-R7943 in this study were consistent with the general characteristics of those for NCX1-, NCX2-, and NCX3-isoform genes transfected into CCL39 cells (23). However, in this study, NCX in odontoblasts showed slight sensitivity to SEA0400. It was found that SEA0400 predominantly blocked NCX1, only mildly blocked NCX2, and exerted almost no influence on NCX3 (22, 24). Although KB-R7943 inhibited all NCX isoforms, KB-R7943 was 3 times more effective against NCX3 than against NCX1 or NCX2 (22, 23). In odontoblasts in this study, the inhibitory potencies against Ca^{2+} influx by reverse exchange were KB-R7943 > SEA0400. Therefore, together with the results from immunohistochemical analysis, the partial inhibitory effect of these inhibitors on Ca^{2+} influx by NCX indicates the expression of both

NCX1 and NCX3 in odontoblasts. In addition, our results showed that the expression potencies of odontoblast NCX isoforms were NCX3 > NCX1.

The values for the equilibrium binding constant (0.4 mmol/L) for Ca^{2+}-dependent reverse-exchange and the apparent dissociation constant (44 mmol/L) for Na^+-dependent forward-exchange in odontoblasts were in line with values reported for reverse and forward Na^+-Ca^{2+} exchange in mammalian cells (2, 21, 25). In addition, these values fell within the range of those for Na^+ and Ca^{2+} concentrations in dentinal fluid at the dentin mineralizing front; concentrations in dentinal fluid for Na^+ and Ca^{2+} were 33–48 mmol/L and 0.7–1.0 mmol/L, respectively (26, 27). These results indicated that odontoblast NCX is potentially active under normal physiologic conditions. Note that the extracellular Ca^{2+} activity has been reported to be 2–3 times higher in the predentin region (pCa = 2.94) than in dental pulp (pCa = 3.37) (27). Na^+ concentrations are lower (33–48 mmol/L) in dentinal fluid at the dentin-forming site than in serum (145 mmol/L). Taken together with our results, this indicates the existence of Na^+ incorporation mechanism that couples with Ca^{2+} extrusion via Na^+-Ca^{2+} exchange in odontoblasts. This system acts as a Ca^{2+} extrusion pathway by using the transmembrane Na^+ gradient, resulting in a lower concentration of Na^+ at the mineralizing front of the predentin region.

It has been reported that NCX is positioned along the surface of osteoblasts, adjacent to the site of bone formation (28). The distribution of NCX in osteoblasts suggests that NCX plays an important role in regulating transport of bone fluid Ca^{2+} for mass mineralization of the bone matrix (9, 29). Although we observed immunoreaction to NCX1 and NCX3 throughout the cell membrane in this study, NCX1 and NCX3 were intensively localized on the distal membrane of the odontoblasts. This suggests that expression of NCX1 and NCX3 in odontoblasts plays an important role in the Ca^{2+} extrusion mechanism, mostly in transportation of Ca^{2+} to the mineralizing front, while maintaining $[Ca^{2+}]_i$ levels.

During dentin formation, Ca^{2+} is transferred from the vascular network across the odontoblast cell layer for incorporation into the mineralizing front (7, 8). Odontoblasts have been suggested to play a central role in this ion transport, in that Ca^{2+} is transported through the cells themselves by different transmembraneous ion-transporting mechanisms (15). Taken together with the results of these earlier reports, this suggests that the membrane proteins in odontoblasts serve as a directional transcellular Ca^{2+} transporting pathway from the circulation to the mineralizing front. In a previous study, we demonstrated that odontoblasts expressed at least 3 phospholipase C (PLC)–coupled receptors that were activated by extracellular signaling molecules released by inflammatory (bradykinin receptors and ATP-binding metabotropic P2Y purinoreceptors) or cholinergic (muscarinic-cholinergic receptors) responses in dental pulp (10). Activation of these PLC-coupled receptors elicited inositol 1,4,5-triphosphate (IP_3)–induced Ca^{2+} release and subsequent store-operated Ca^{2+} channel opening after depletion of IP_3-sensitive Ca^{2+} stores (10). In addition, depolarization activated a spontaneous $[Ca^{2+}]_i$ increase (Ca^{2+} oscillation) in odontoblasts mediated by Ca^{2+}-induced Ca^{2+} release after activation of voltage-dependent Ca^{2+} channels (12). Recently, we demonstrated Ca^{2+} entry via transient receptor potential vanilloid channels (TRPV1–TRPV4) in odontoblasts (14, 30), which essentially contribute to thermosensitive sensory transmission. The present results suggest that the excessive internal Ca^{2+} induced by these Ca^{2+} mobilization pathways was extruded via NCX in odontoblasts to regulate intracellular Ca^{2+} levels. In addition, this Ca^{2+} extrusion mechanism via NCX at the distal membrane of odontoblasts might serve as a directional Ca^{2+} transport pathway from the circulation to the dentin-mineralizing front by transporting accumulated intracellular Ca^{2+} resulting from accelerated Ca^{2+} signaling events activated by physiologic/pathophysiologic dental pulp responses or by stimuli external to the dentin.

Acknowledgments

This work was supported by a MEXT HAITEKU (2004, 2006) Project (HRC7, HRC6A03), Grant-in-Aid (No. 18592050/20592187) for Scientific Research from the MEXT of Japan, a Grant from the Dean of the Tokyo Dental College, and a grant for special expenses for graduate schools from the MEXT of Japan. We would like to thank Associate Professor Jeremy Williams, Tokyo Dental College, for his invaluable assistance with the English language used in this manuscript.

References

1. Matsuda T, Takuma K, Baba A. Na^+-Ca^{2+} exchanger: physiology and pharmacology. Jpn J Pharmacol 1997;74:1–20.
2. Blaustein MP, Lederer WJ. Sodium/calcium exchange: its physiological implications. Physiol Rev 1999;79:763–854.
3. Philipson KD, Nicoll DA, Ottolia M, et al. The Na^+/Ca^{2+} exchange molecule: an overview. Ann N Y Acad Sci 2002;976:1–10.
4. Quednau BD, Nicoll DA, Philipson KD. The sodium/calcium exchanger family-SLC8. Pflugers Arch 2004;447:543–8.
5. Quednau BD, Nicoll DA, Philipson KD. Tissue specificity and alternative splicing of the Na^+/Ca^{2+} exchanger isoforms NCX1, NCX2, and NCX3 in rat. Am J Physiol 1997; 272:C1250–61.
6. Lundgren T, Linde A. Na^+/Ca^{2+} antiports in membranes of rat incisor odontoblasts. J Oral Pathol 1988;17:560–3.
7. Linde A. Dentin mineralization and the role of odontoblasts in calcium transport. Connect Tissue Res 1995;33:163–70.
8. Linde A, Lundgren T. From serum to the mineral phase: the role of the odontoblast in calcium transport and mineral formation. Int J Dev Biol 1995;39:213–22.
9. Lundquist P, Lundgren T, Gritli-Linde A, Linde A. Na^+/Ca^{2+} exchanger isoforms of rat odontoblasts and osteoblasts. Calcif Tissue Int 2000;67:60–7.
10. Shibukawa Y, Suzuki T. Ca^{2+} signaling mediated by IP_3-dependent Ca^{2+} releasing and store-operated Ca^{2+} channels in rat odontoblasts. J Bone Miner Res 2003; 18:30–8.
11. Lundgren T, Linde A. Voltage-gated calcium channels and nonvoltage-gated calcium uptake pathways in the rat incisor odontoblast plasma membrane. Calcif Tissue Int 1997;60:79–85.
12. Shibukawa Y, Suzuki T. Measurements of cytosolic free Ca^{2+} concentrations in odontoblasts. Bull Tokyo Dent Coll 1997;38:177–85.
13. Shibukawa Y, Suzuki T. Ionic currents in odontoblasts and dental pulp cells. In: Nakamura Y, Sessle BJ, eds. Neurobiology of mastication: from molecular to systems approach. Amsterdam: Elsevier Science BV; 1999:165–8.
14. Okumura R, Shima K, Muramatsu T, et al. The odontoblast as a sensory receptor cell?: the expression of TRPV1 (VR-1) channels. Arch Histol Cytol 2005;68: 251–7.
15. Linde A, Lundgren T. Calcium transport in dentinogenesis. J Biol Buccale 1990;18: 155–60.
16. Shibukawa Y, Suzuki T. A voltage-dependent transient K^+ current in rat dental pulp cells. Jpn J Physiol 2001;51:345–53.
17. Hamill OP, Marty A, Neher E, Sakmann B, Sigworth FJ. Improved patch-clamp techniques for high-resolution current recording from cells and cell-free membrane patches. Pflugers Arch 1981;391:85–100.
18. Matsuda T, Arakawa N, Takuma K, et al. SEA0400, a novel and selective inhibitor of the Na^+-Ca^{2+} exchanger, attenuates reperfusion injury in the in vitro and in vivo cerebral ischemic models. J Pharmacol Exp Ther 2001;298:249–56.
19. Min KS, Lee HJ, Kim SH, et al. Hydrogen peroxide induces heme oxygenase-1 and dentin sialophosphoprotein mRNA in human pulp cells. J Endod 2008; 34:983–9.
20. Maciejewska I, Cowan C, Svoboda K, Butler WT, D'Souza R, Qin C. The NH2-terminal and COOH-terminal fragments of dentin matrix protein 1 (DMP1) localize differently in the compartments of dentin and growth plate of bone. J Histochem Cytochem 2009;57:155–66.
21. Schnetkamp PP. The SLC24 Na^+/Ca^{2+}-K^+ exchanger family: vision and beyond. Pflugers Arch 2004;447:683–8.
22. Iwamoto T. Forefront of Na^+/Ca^{2+} exchanger studies: molecular pharmacology of Na^+/Ca^{2+} exchange inhibitors. J Pharmacol Sci 2004;96:27–32.

23. Iwamoto T, Shigekawa M. Differential inhibition of Na^+/Ca^{2+} exchanger isoforms by divalent cations and isothiourea derivative. Am J Physiol 1998;275:C423–30.
24. Iwamoto T, Kita S, Uehara A, et al. Molecular determinants of Na^+/Ca^{2+} exchange (NCX1) inhibition by SEA0400. J Biol Chem 2004;279:7544–53.
25. Kang KJ, Shibukawa Y, Szerencsei RT, Schnetkamp PP. Substitution of a single residue, Asp575, renders the NCKX2 K^+-dependent Na^+/Ca^{2+} exchanger independent of K^+. J Biol Chem 2005;280:6834–9.
26. Larsson PA, Howell DS, Pita JC, Blanco LN. Aspiration and characterization of predentin fluid in developing rat teeth by means of a micropuncture and microanalytical technique. J Dent Res 1988;67:870–5.
27. Lundgren T, Nannmark U, Linde A. Calcium ion activity and pH in the odontoblast-predentin region: ion-selective microelectrode measurements. Calcif Tissue Int 1992;50:134–6.
28. Stains JP, Weber JA, Gay CV. Expression of Na^+/Ca^{2+} exchanger isoforms (NCX1 and NCX3) and plasma membrane Ca^{2+} ATPase during osteoblast differentiation. J Cell Biochem 2002;84:625–35.
29. Stains JP, Gay CV. Inhibition of Na^+/Ca^{2+} exchange with KB-R7943 or bepridil diminished mineral deposition by osteoblasts. J Bone Miner Res 2001;16:1434–43.
30. Son AR, Yang YM, Hong JH, Lee SI, Shibukawa Y, Shin DM. Odontoblast TRP channels and thermo/mechanical transmission. J Dent Res 2009;88:1014–9.